



ELSEVIER

Nuclear Instruments and Methods in Physics Research B 164–165 (2000) 186–190

NIM B
Beam Interactions
with Materials & Atoms

www.elsevier.nl/locate/nimb

Correlation of energy-loss and collected-charge in Si ΔE detectors: Measurements using an Enge spectrometer

Harry J. Whitlow^{a,*}, Yanwen Zhang^{a,1}, Heiko Timmers^b, Trevor R. Ophel^c,
R.G. Elliman^d, Minmei Li^b, D. John O'Connor^b

^a Department of Nuclear Physics, Lund Institute of Technology, Box 118, SE-221 00 Lund, Sweden

^b Department of Physics, University of Newcastle, Callaghan, NSW 2308, Australia

^c Department of Nuclear Physics, Research School of Physical Sciences, Australian National University, Canberra, ACT 0200, Australia

^d Department of Electronic Materials Engineering, Research School of Physical Sciences, Australian National University, Canberra, ACT 0200, Australia

Abstract

The correlation between energy-loss and collected-charge for individual ions traversing 7.1 μm self-supporting Si p-i-n ΔE detectors has been studied using the Enge spectrometer at the Australian National University. In this work the simultaneous measurements of the ΔE signal and energy-loss were made for 49 MeV ^{28}Si and 103 MeV ^{28}Si and 147 MeV ^{74}Ge incident ions obtained by 10° scattering of a primary beam from a thin gold target supported on a carbon foil. The results show that there exists a strong correlation (correlation coefficient $r \sim 0.9$) between the individual ions energy-loss and the collected-charge signal. Consequently the distributions of collected-charge and energy-loss are closely similar. The energy-loss distributions exhibit high energy-loss tails that may be attributed to asymmetry in the distribution of electronic energy-loss and/or to trajectory length spreading as a result of single and multiple scattering in nuclear collisions. © 2000 Elsevier Science B.V. All rights reserved.

PACS: 34.50.Bw; 29.40.-n; 61.82.Fk; 29.40.Aj

Keywords: ΔE detector; Energy loss; Enge spectrometer; Si detectors; Energy straggling; Multiple scattering; Charge state

1. Introduction

The advent of extremely thin Si detectors (extending to 1 μm and below) through which ions with less than about 1 MeV per nucleon energy can traverse, opens up new experimental possibilities for the study of energy-loss phenomena in matter. They may be used as active stopping media (e.g. for study of the p and \bar{p} Barkas effect [1]) and as active channelling targets. Neutral- and

* Corresponding author. Tel.: +46-46-222-7630; fax: +46-46-222-4709.

E-mail address: harry_j.whitlow@nuclear.lu.se (H.J. Whitlow).

¹ Present address: Division of Ion Physics, The Ångström Laboratory, Box 534, SE-751 21, Uppsala, Sweden.

charge-state inclusive measurements with Si detectors can also contribute to developing an understanding of the detailed mechanisms in which energy deposited by energetic ions is coupled to electron–hole production [2–5].

It has been previously shown that for polyenergetic light projectiles with $Z_1 \leq 8$, the charge collected from a Si p–i–n ΔE detector has a linear dependence on the energy loss in the ΔE detector [5]. The objective of this work is to investigate the relationship between the collected-charge signal and the energy-loss in the detector in the limit of monoenergetic incident ions where the energy-loss broadening is solely associated with the stochastic nature of the energy-loss processes in the ΔE detector. The correlation between the electrical collected-charge signal and energy-loss in this limit provides information about the stochastics of charge carrier collection from the plasma column along the ion track.

2. Experimental

The experimental configuration employed is shown in Fig. 1. The 14 UD Pelletron accelerator at ANU was used to provide beams of 50.4 $^{28}\text{Si}^{7+}$, 104 MeV $^{28}\text{Si}^{8+}$ and 150 MeV $^{74}\text{Ge}^{11+}$ ions (Table 1). The incident ions were scattered through 10° by a thin Au film on a supporting $\sim 35 \mu\text{g cm}^{-2}$ C film. The same self-supporting Si detector [6,7] as used for our previous studies [5] was mounted so it could be moved into and out of the path of scattered ions entering the entrance slits of the Enge spectrometer. The ΔE detector was heated at 120°C for 4 h prior to mounting in order to restore

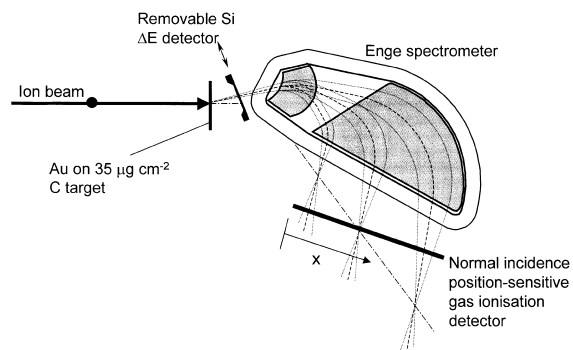


Fig. 1. Schematic illustration of the experimental configuration. (Enge spectrometer details after Enge [10]). The spreading of off-axis ion trajectories is exaggerated for clarity and the density of grey indicates the regions with greater magnetic field strength.

the leakage current and minimise the effect of radiation damage [8]. The geometrical thickness of the detector was $7.1 \mu\text{m}$ and the dead layers were estimated to be 600 and 500 nm on the front and rear faces, respectively. These values are in good agreement with estimates based on the capacitance for total depletion and the known thickness of the front and rear contact regions. To minimise positional spreading associated with scattering of the ions in the entrance window of the gas detector, the ANU Enge spectrometer [9–15] was operated with an out-of-focal-plane position-sensitive gas ionisation detector [9] so that the ions impinged normally.

The measurements were carried out in two steps. In the first step the ΔE detector was removed from the ion path in order to calibrate the Enge spectrometer. The energy E of an ion was related

Table 1
Incident and scattered ion energies and charge states with moments of the energy-loss and ΔE distribution moments

Ion	E_0^a (MeV)	q_0	E_1^a (MeV)	q_2	$\langle EL^1 \rangle$ (MeV)	$\langle \Delta EL^2 \rangle^{1/2}$ (MeV)	σ_{trend}^b (MeV)	r^c
^{28}Si	50.037	7+	49.229	8+	26.92	0.761	0.138	+0.977
^{28}Si	103.789	8+	102.888	12+	21.64	3.394	0.168	+0.995
^{74}Ge	150.141	11+	146.781	18+	62.79	2.051	0.347	+0.894

^a Assigned energy values from N.M.R. probes.

^b The variance of the data points perpendicular to the trend line.

^c The correlation coefficient between the EL and ΔE signals.

to the position signal (X) from the gas detector according to

$$E = K_{\text{Au}}E_0 - \Delta E_{\text{foil}} = \frac{f_1^2 q_1^2}{M} k(X_1), \quad (1)$$

where K_{Au} is the kinematic factor for scattering of the ions at 10° , E_0 the incident ion energy and ΔE_{foil} is the energy lost in the carbon foil, f_1 is the frequency of the Nuclear Magnetic Resonance (NMR) field probe and q_1 and M are the ions' charge state and mass, respectively. Here the subscript 0 refers to the incident ion beam and the subscript 1 denotes that the ΔE detector is not in the path of the scattered ions. $k(X_1)$ is the calibration constant of the magnet corresponding to the position signal X_1 which was calibrated against the NMR probe frequency of the analysing magnet from measurements of the position signal for a fixed charge state as the accelerator energy was varied in small steps. The first moment of the position signal distributions was obtained by fitting Pearson-V distribution lineshapes. It was found that $k(X)$ could be represented as a polynomial:

$$k(X) = 0.0106558 + 9.109919X + 1.07 \times 10^{-10}X^2. \quad (2)$$

The best condensation of the calibration data onto a single line was achieved when the C-foil thickness was taken to be $35 \mu\text{g cm}^{-2}$ rather than the nominal thickness of $20 \mu\text{g cm}^{-2}$ as stated by the manufacturer.

In the second stage of the measurements the ΔE detector was moved into the path of the ions and the collected-charge (ΔE) signal was recorded in coincidence with the position signal from the Enge spectrometer. During these measurements the leakage current of the detector increased slightly from 170 to 180 nA. The energy loss EL of each ion is then

$$EL = K_{\text{Au}}E_0 - \Delta E_{\text{foil}} - \frac{f_2^2 q_2^2}{M} k(X_2). \quad (3)$$

Here, the subscript 2 denotes that the ΔE detector is in the path of the scattered ions.

The charge states q_2 of the ions exiting the ΔE detector were assigned by comparing the energy

loss estimated from SRIM-2000 [16,17] with the measured EL values. The search criteria were such that the mean EL deviated by less than $\pm 20\%$ from the SRIM-2000 estimate and the energy-loss had the correct energy dependence. An essential assumption is that the ΔE detector is sufficiently thick so that the quasi-equilibrium charge-state distribution is attained and thus EL is independent of the entrance q_1 and exit q_2 charge states.

3. Results and discussion

Fig. 2 presents the correlation between EL and the collected-charge signal from the ΔE detector for 146.8 MeV $^{74}\text{Ge}^{18+}$ ions. The calibration of the ΔE signal in Fig. 2 in MeV was established from the trend line [5]. The energy span per channel in the ΔE signal obtained from the trend line was 7.2% larger than that estimated from SRIM-2000 [16] and the channel number corresponding to the position of the peaks in the ΔE spectra.

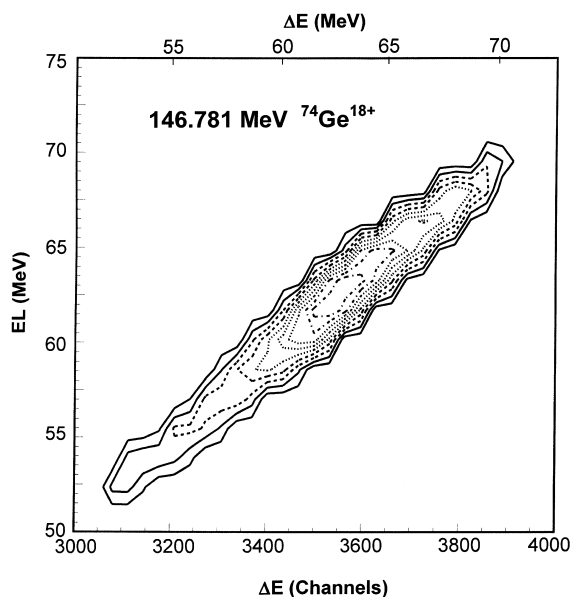


Fig. 2. Correlation between ΔE signal measured by the detector and energy-loss EL of 146.781 MeV $^{74}\text{Ge}^{18+}$ ions traversing a $7.1 \mu\text{m}$ thick Si p-i-n detector. The ΔE scale in MeV units has been assigned from the trend line. The contour scale denotes 10 logarithmically spaced levels.

The positive correlation between EL and the ΔE channel number is seen in Fig. 2 and the correlation coefficient $r \sim +0.9$, or greater (Table 1), implies that the dominating contribution to the broadening of the ΔE signal is associated with the stochastic nature of the energy-loss of ions traversing the detector. Similar results were obtained for 49.2 and 102.9 MeV ^{28}Si ions. Comparison of the r.m.s. deviation $\langle \Delta EL^2 \rangle^{1/2}$ of the data points about the mean energy-loss $\langle EL \rangle$ with the r.m.s. perpendicular deviation of the data points from the trend line σ_{trend} (Table 1) reveals that σ_{trend} is 5–18% of $\langle \Delta EL^2 \rangle^{1/2}$. These results imply that for the ions investigated here, the stochastic broadening associated with charge carrier collection from the plasma column is a small contribution to the ΔE signal lineshape and the ΔE detectors may be used as active stopping media.

σ_{trend} is the geometric mean of the uncertainties σ_{EL} and $\sigma_{\Delta E}$ in determining EL and ΔE , respectively for an individual ion. $\sigma_{\Delta E}$ is associated with the variability in charge carrier collection and electronic noise contributions. σ_{EL} , the broadening associated with EL , is the geometric sum of the uncertainties in determining E_1 and E_2 , the energies of an ion entering and leaving the ΔE detector, respectively. Detailed estimation of σ_{EL} is non-trivial because it involves beam broadening, kinematic broadening and straggling in the C-foil and the uncertainty in energy measurement with the spectrometer for charge state q_2 . However, a simple estimate can be obtained using the width of the E_1 for charge states q_1 which was 0.125, 0.242 and 0.243 MeV for 49.2 MeV $^{28}\text{Si}^{12+}$, 102.9 MeV $^{28}\text{Si}^{13+}$ and 146.8 MeV $^{74}\text{Ge}^{24+}$, respectively. These widths represent upper limits to σ_{EL} because the contribution to these widths from the Enge spectrometer will be reduced in scaling to charge state q_2 . Comparison with Table 1 suggests that it is thus highly likely that the chief contribution to σ_{trend} originates from the uncertainty in determination of the energy loss and not from $\sigma_{\Delta E}$.

Fig. 3 presents the superposed ΔE signal and energy loss spectra for 49.2 MeV $^{28}\text{Si}^{9+}$, 102.9 MeV $^{28}\text{Si}^{12+}$ and 146.8 MeV $^{74}\text{Ge}^{18+}$ ions. The ΔE signal in Fig. 3 was converted to MeV using the slope and intercept of the trend line from the correlation analysis. A correction was applied to

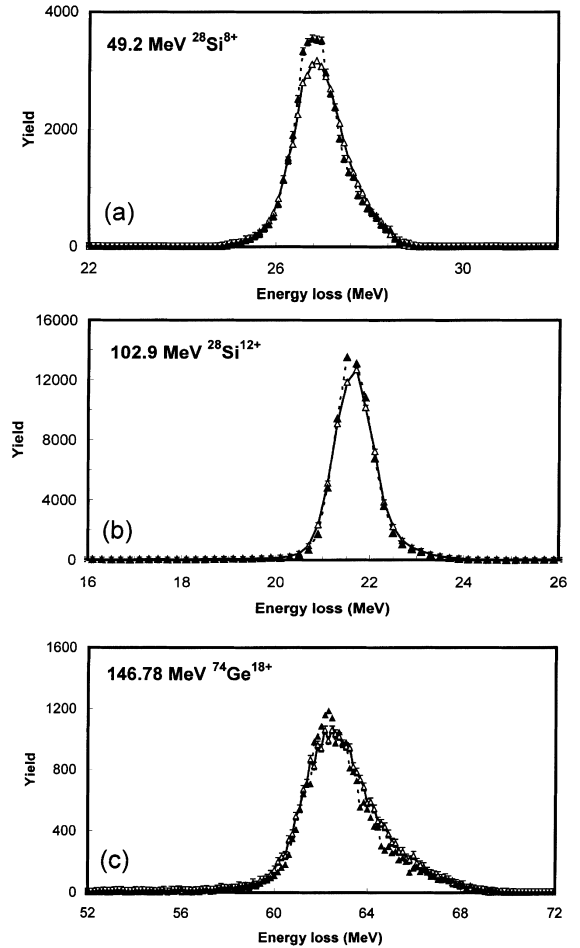


Fig. 3. ΔE (filled triangles) and EL (open triangles) distributions for 49.2 MeV ^{28}Si , 102.9 MeV ^{28}Si and 146.8 MeV ^{74}Ge ions, respectively. The data has been normalised and the ΔE signal calibrated as described in the text.

the energy-loss distribution to remove the effect of variation in the ratio of EL - to X -bin spans, $\delta EL/\delta X$, which follow from Eqs. (2) and (3). The effect of this correction turned out to have a negligible effect on the shape of EL distribution because the peaks spanned only a small range of X . This procedure normalises distribution moments lower than second-order. It will thus act to make the broader distribution appear more sharply peaked than the narrower distribution. We note that the calibration procedure may modify the odd order moments, however, it will not introduce

skewness if it was not present in the original distribution.

For all the ions investigated *both* EL and ΔE distributions are skewed with pronounced tails extending towards greater EL values (Fig. 3). It is interesting to consider possible origins of the skewness. From Table 1 it can be seen that a considerable fraction (40–60%) of the scattered ion energy is deposited in the ΔE detector. Thus we are dealing with a thick stopping media where the charge state distributions which govern the energy-loss and straggling [17–19] should be well established. The nuclear scattering contribution to energy-loss at these energies is negligible. It follows from the fact that the tail is observed in both the ΔE and EL distributions that the tail is associated with skewness in the electronic energy-loss distribution and not from the charge carrier collection effects or directly from nuclear stopping. This might be associated with intrinsic skewness in the electronic energy-loss distribution [20]. Another contribution to skewness may be associated with the fraction of ions that have undergone nuclear scattering. For ions normally incident on the detector those ions that do not undergo nuclear scattering will have the shortest path, and hence smallest electronic energy-loss in the ΔE detector. On the other hand ions that undergo nuclear scattering will have systematically longer paths through the detector as a result of the angular deviation, and hence experience a larger electronic energy-loss.

4. Conclusions

For the ions investigated here:

1. The electrical ΔE signal from a thin ΔE detector is closely correlated with the energy deposited by the ion in question within the ΔE detector.
2. The broadening and skewness of the lineshape of the ΔE signal from the detector is dominated by the contributions from the energy-loss process.
3. The small contribution to the ΔE lineshape from stochastic processes in collection of the charge carriers implies thin Si ΔE detectors are well suited as active stopping media for neutral and charge-state inclusive measurements of the energy deposited by individual ions.

Acknowledgements

The Royal Physiographic Society in Lund is warmly thanked for travel support.

References

- [1] S.P. Møller, Nucl. Instr. and Meth. B 48 (1990) 1.
- [2] W.N. Lennard, K.B. Winterbon, Nucl. Instr. and Meth. B 24/25 (1987) 1035.
- [3] W.N. Lennard, H. Geissel, K.B. Winterbon, D. Philips, T.K. Alexander, J.S. Forster, Nucl. Instr. and Meth. A 248 (1986) 454.
- [4] D. Comedi, J. Davies, Nucl. Instr. and Meth. B 67 (1992) 93.
- [5] Y. Zhang, H.J. Whitlow, T. Winzell, Nucl. Instr. and Meth. B 159 (1999) 101.
- [6] H.J. Whitlow, T. Winzell, G. Thungström, Nucl. Instr. and Meth. B 136–138 (1998) 616.
- [7] L. Evensen, T. Westgaard, V. Avdeichikov, L. Carlén, B. Jakobsson, Y. Murin, J. Mårtensson, A. Oskarsson, A. Siwek, H.J. Whitlow, E.J. van Veldhuizen, L. Westerberg, M. Guttormsen, IEEE Trans. Nucl. Sci. 44 (1997) 629.
- [8] H.J. Whitlow, S.J. Roosendaal, M. El Bouanani, R. Ghetti, P.N. Johnston, B. Jakobsson, R. Hellborg, H. Petersson, P. Omling, Z. Wang, CHIC Collaboration, Nucl. Instr. and Meth. B 135 (1998) 523.
- [9] T.R. Ophel, L.K. Fifield, W.N. Catford, N.A. Orr, C.L. Woods, A. Harding, G.P. Clarksson, Nucl. Instr. and Meth. A 272 (1988) 734.
- [10] H.A. Enge, Nucl. Instr. and Meth. 28 (1964) 119.
- [11] J.E. Spencer, H.A. Enge, Nucl. Instr. and Meth. 49 (1967) 181.
- [12] T.R. Ophel, A. Johnston, The Enge Spectrograph and Focal Plane Detection System, Australian National University, Research School of Physical Sciences, ANU-P/680, 1977.
- [13] T.R. Ophel, A. Johnston, Nucl. Instr. and Meth. 157 (1978) 461.
- [14] J.R. Leigh, T.R. Ophel, Nucl. Instr. and Meth. 192 (1982) 615.
- [15] W.N. Catford, L.K. Fifield, M.A.C. Hotchkis, T.R. Ophel, N.A. Orr, D.C. Weisser, C.L. Woods, Nucl. Instr. and Meth. A 260 (1987) 146.
- [16] J.F. Ziegler, TRIM v.06 from SRIM-2000 program package. obtainable from: <http://www.research.ibm.com/ion-beams/home.htm#SRIM>.
- [17] J.F. Ziegler, J.P. Biersack, U. Littmark, The Stopping and Ranges of Ions in Matter, Vol. 1, Pergamon Press, New York, 1985.
- [18] P. Sigmund, L. Glazov, Nucl. Instr. and Meth. B 136–138 (1998) 47.
- [19] P. Sigmund, Nucl. Instr. and Meth. B 135 (1998) 1.
- [20] L. Glazov, P. Sigmund, To be published.